Quantum Well Hall Effect Sensor Based Handheld Magnetic Scanner with Programmable Electromagnetic Coil for Non-Destructive Testing of Ferromagnetic and Non-Ferromagnetic Materials

Authors:
Firew Abera Biruu MEng MIET
Dr Ertan Balaban
Dr Ehsan Ahmad
Professor Mohamed Missous

University of Manchester

55th Annual Conference of the British Institute for Non-Destructive Testing
Nottingham, United Kingdom
September 2016

MANCHESTER 1824
The University of Manchester

Talk Outline

- Introduction
- QWHE Sensors
- Design and Fabrication of a proposed Handheld Scanner
- Preliminary Test Results
- Conclusion

MANCHESTER 1824
The University of Manchester

Introduction

Defects in engineering materials happen at anytime during their life span in sizes not visible to human eye. Due to this, they can progress undetected, without specialist monitoring or testing devices, to cause catastrophic failure of a given system.

Most relevant testing methods studied here are non destructive and provide an invaluable alterative to destructive testing systems, where a material undergoes intentional destruction and could not be recovered. Such testing devices relate to particular scientific principles. Likewise, testing systems studied here are based on electromagnetic principles.

Beside their positive advantages and unique solution to materials testing, some of these methods are bulky and use hazardous chemicals. Some systems, like silicon based Hall effect sensors have low sensitivities and consume high power.

Introduction

A new approach that is already ongoing at the University of Manchester is the use of a new class of extremely sensitive Hall Effect sensors called Quantum Well Hall Effect (QWHE) sensors to detect stray (nanoTesla) magnetic field signatures.

The research presented here has the potential to contribute greatly to future NDT and contactless sensing systems.

Quantum Well Hall Effect Sensors

QWHE sensors:

- Have higher sensitivities than commercial alternatives
- Operate on a very wide dynamic range of field

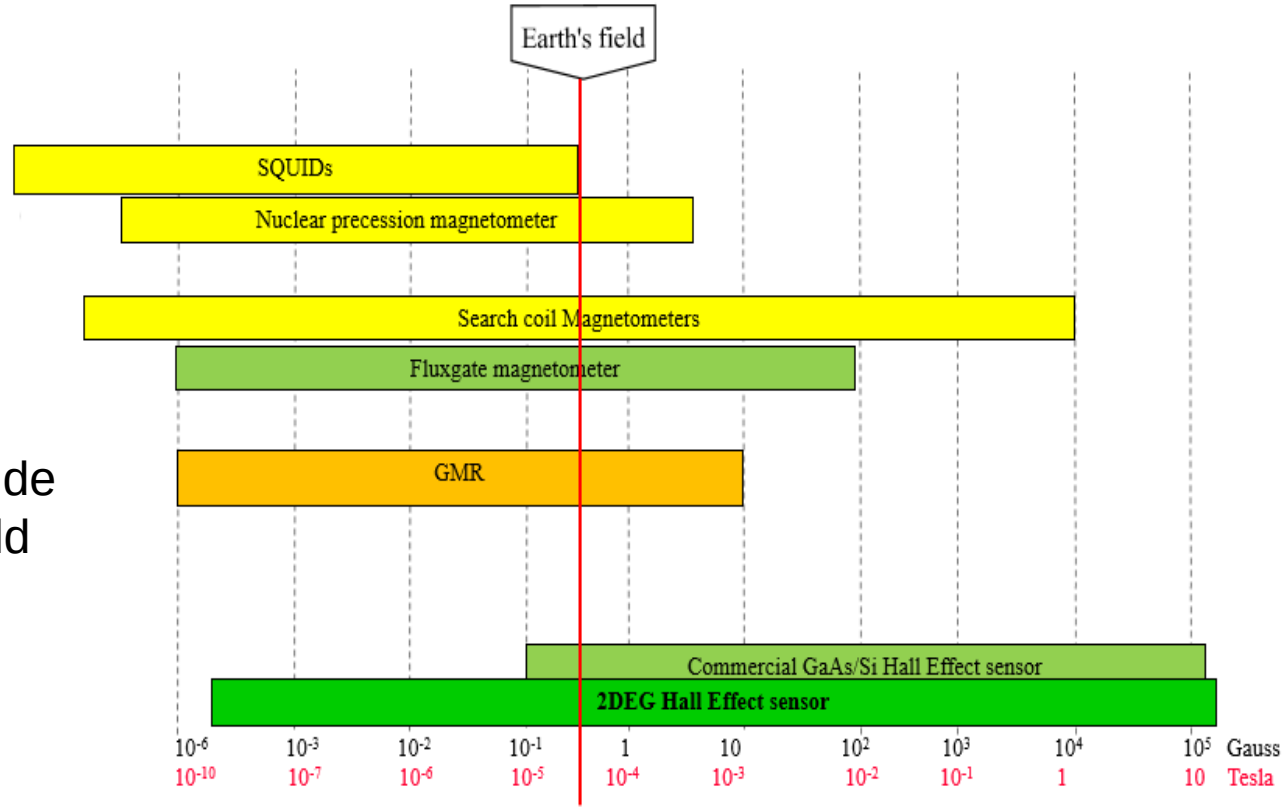

Fig 5. Magnetic field sensor spectrum: > 10^{10}

MANCHESTER 1824
The University of Manchester

2D Magnetic Fields Imaging

Many devices have been developed to inspect defects based on electromagnetic principles.

Present technologies perform a one dimensional magnetic field measurement. Methods like MFL and ACFM are usually performed separately.

The possibility of capturing 2D magnetic field data would help to investigate the defect more deeply. Integrating a programmable magnetic field illumination source helps to perform both MFL and ACFM like techniques allowing both magnetic and non magnetic materials to be inspected.

Design and Fabrication

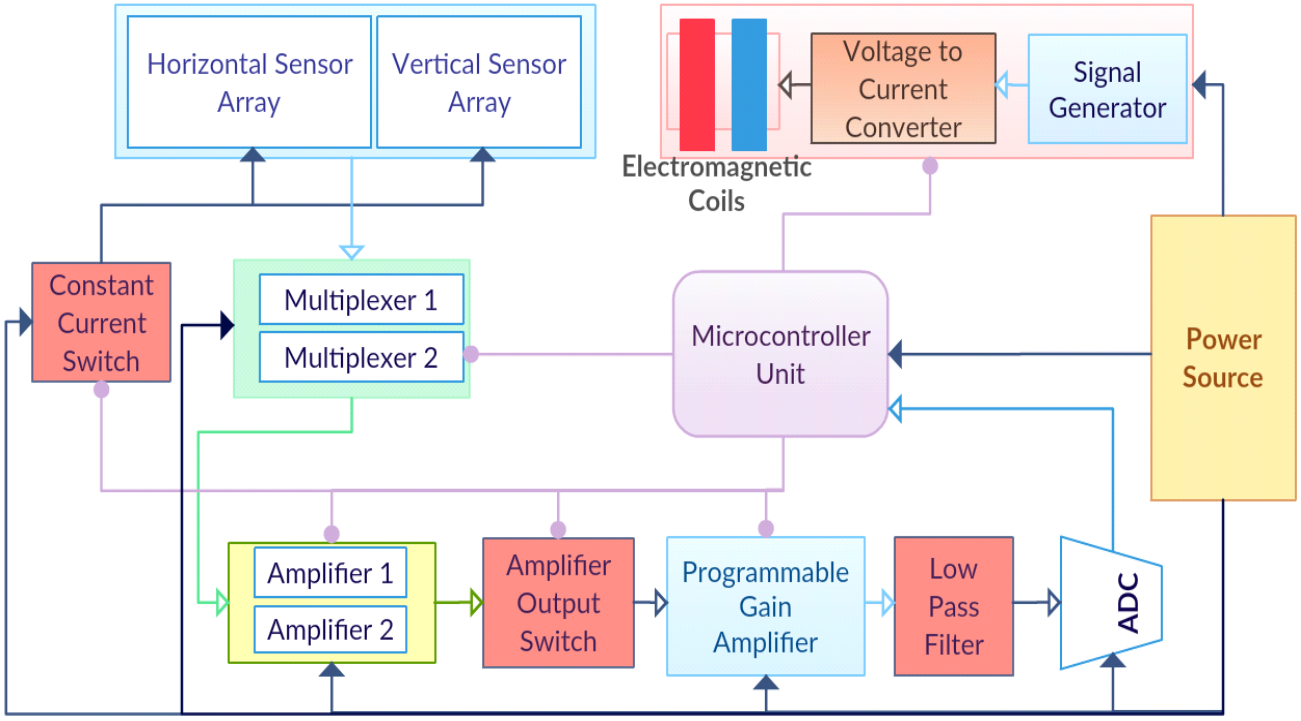

Fig 6. Block diagram of Handheld Scanner (HHS)

Design and Fabrication

Sensor Arrays and Orientation

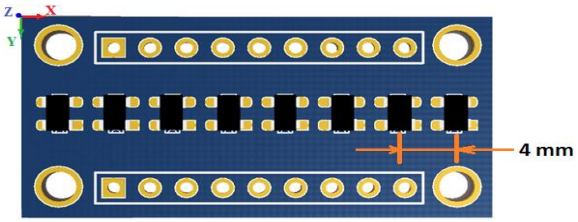

1x8 QWHE sensor array with 4mm pitch

Fig 7. P2A sensor array

Sensors on the horizontal array detect magnetic field normal to the surface of the test piece, B_Z

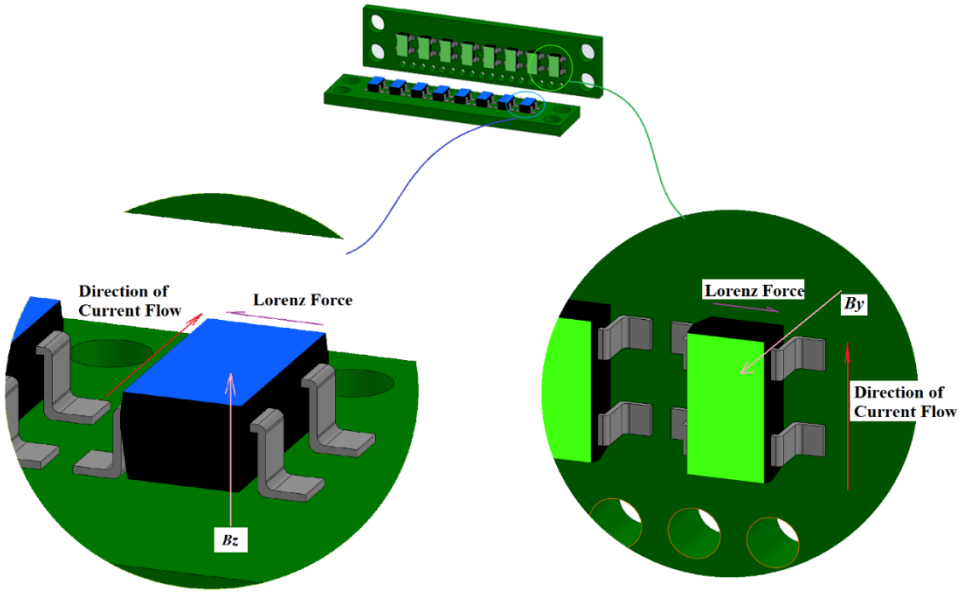

Fig 8. Sensor array orientation

Sensors on the vertical array detect magnetic field parallel to the test piece but perpendicular to B_Z. This magnetic field can either be B_X *or* B_Y

Design and Fabrication

Amplification Gain

$$V_{ADC\_min} = \frac{\Delta V_{ref}}{ADC\ resolution} = \frac{5V}{2^{18}} = 19.07\mu V$$

$$V_H = KBI = 0.17\ \frac{\text{mV}}{\text{mT}\ mA} \times 1mA \times 100nT = 17n\text{V}$$

$$Gain = \frac{V_{ADC\_min}}{V_H} = \frac{19.07\mu V}{17\ nV} = 1121.97$$

$$\approx 1122$$

A fist stage gain of 250 using an INA163A low noise amplifier before switching and a second stage gain of up to 176 is handled by a programmable gain amplifier

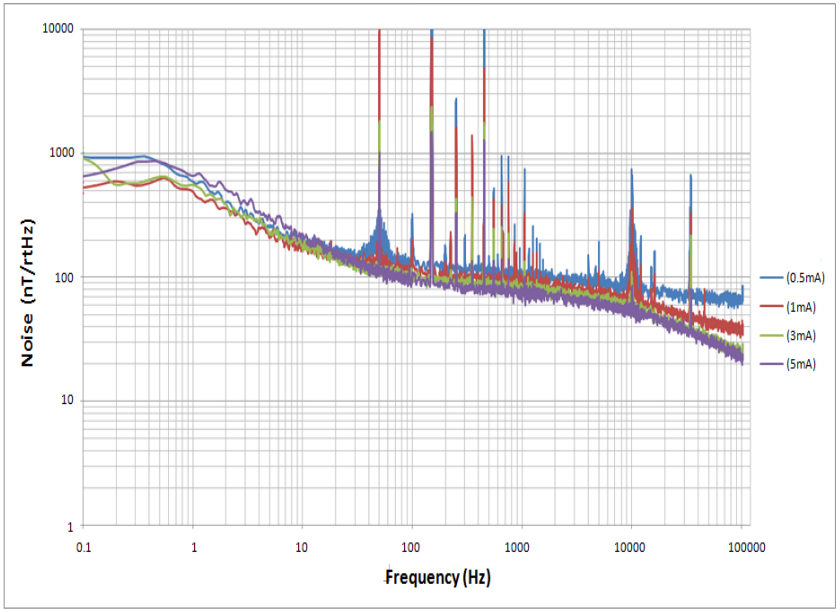

Fig 9. For *1mA* biasing current, the noise floor is 100nT at 10kHz

Design and Fabrication

Design of Electromagnet Coils

The maximum magnetic field that can be generated in the coil, also shown in figure 11, can be calculated from ampere's law, using the calculated effective permeability, as:

$$\mu_{eff} = \frac{2000}{1+(\frac{2\times10^{-3}m}{81.5\times10^{-3}m})2000} = 20.17$$

$$B_{max} = \frac{\mu_0\mu_{eff}NI}{L} = \frac{4\pi\times10^{-7}\times20.17\times31\times3A}{28\times10^{-3}} = 84.18\,mT$$

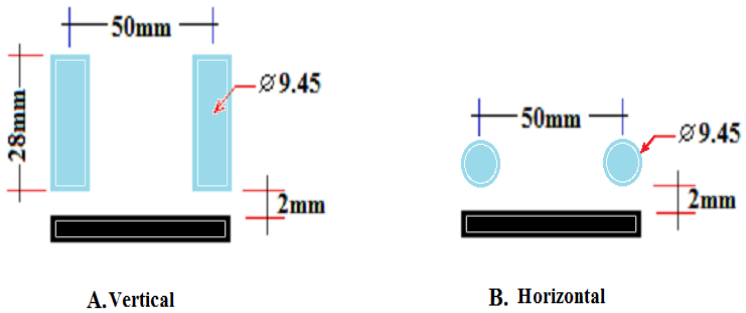

Fig 10. vertical orientation illuminates the test piece with part of the strong internal magnetic field. Left(top): Simulation result, Left(bottom) Programmable Electromagnetic Driver.

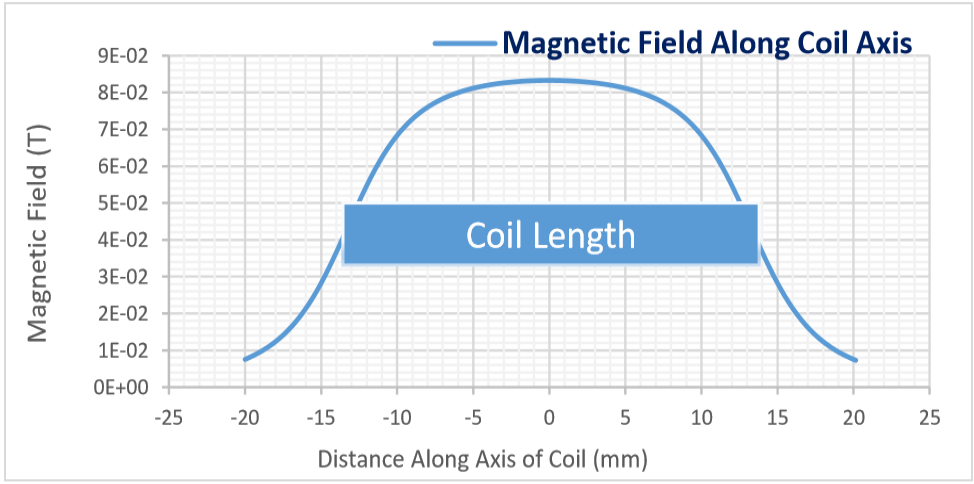

Figure 11. Magnetic Field along the axis of designed electromagnetic coil

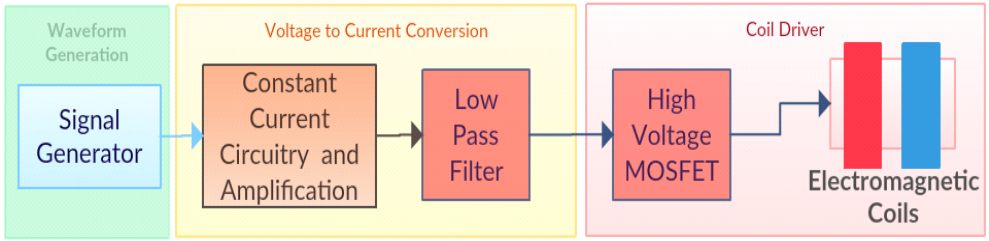

Preliminary Tests

DC Magnetic Field Experimental Test Results

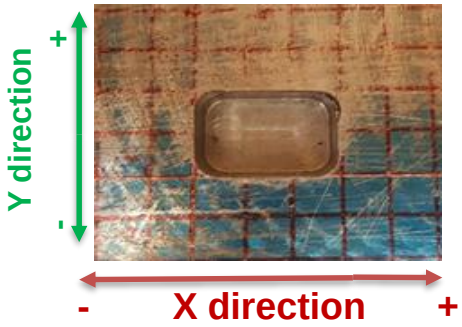

+Z direction perpendicular and out of this page

Coil Parameters

- Wire diameter = 0.71mm (copper)
- Number of turns = 31 per layer
- Number of layers = 3

Test Material

- Material: ferromagnetic steel
- Groove dimension = 15mm x 10mm x 10mm
- Grids shown = 5mm by 5mm

Measurements are taken using QWHE magnetometer

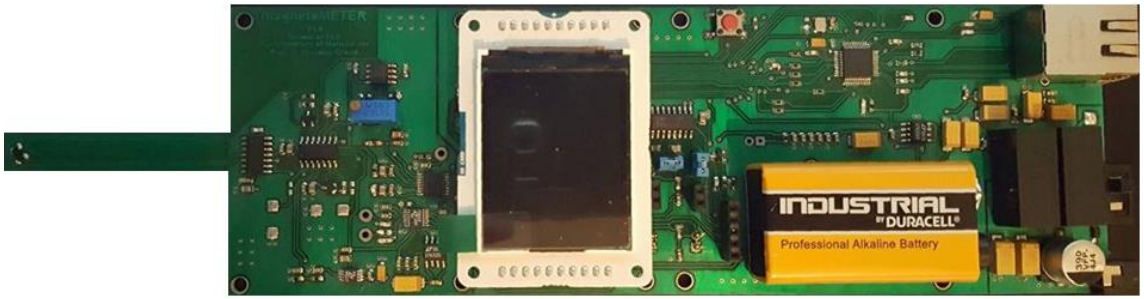

DC Magnetic Field Experimental Test Results

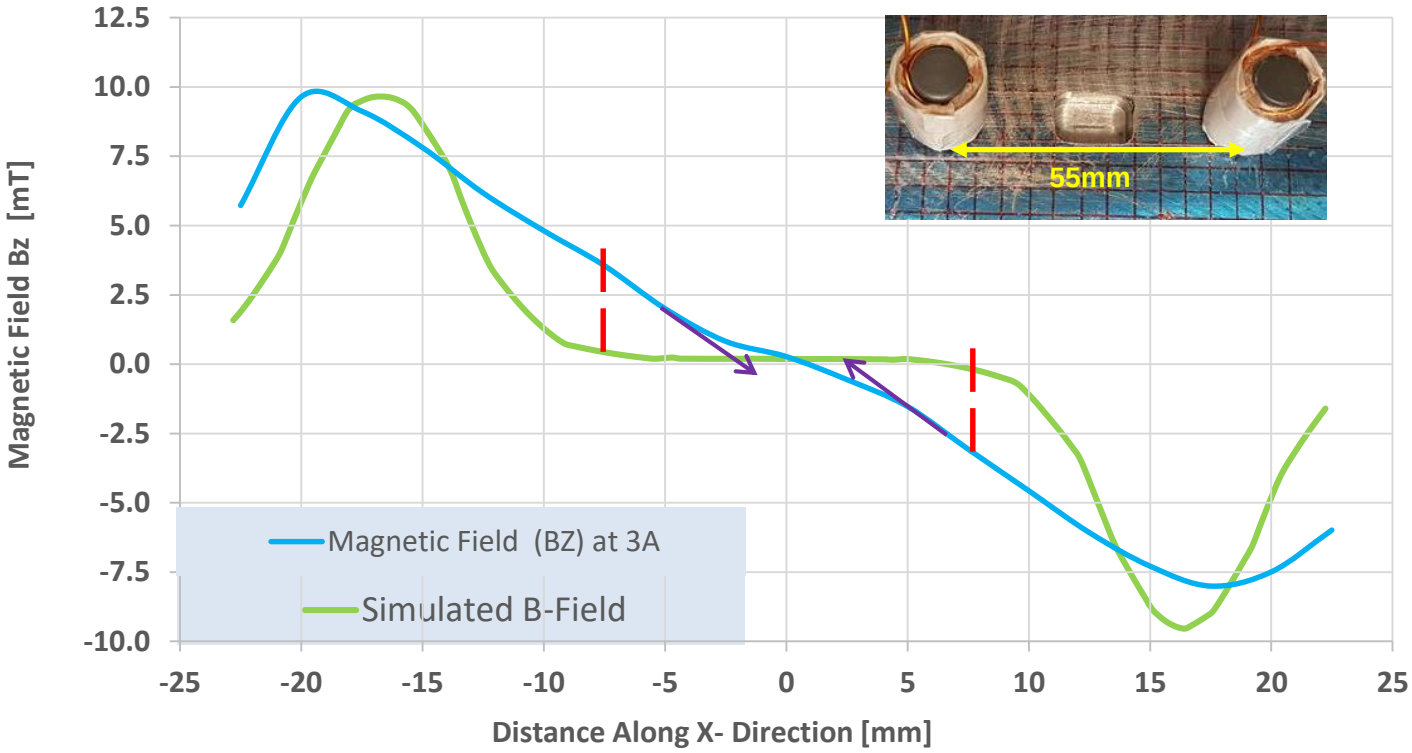

Fig 12. Z Component DC Magnetic Field Measurement

Z-component Magnetic field measurement was made along centre line of the groove in the X-axis direction.

The region in between the red dotted lines is where the actual 'defect' groove is. The existence of the defect is indicated by the experimental curve in blue, which is also accurately shown by simulated curve. The dimension of the groove in the x-axis is an indication of how wide the groove is.

DC Magnetic Field Experimental Test Results

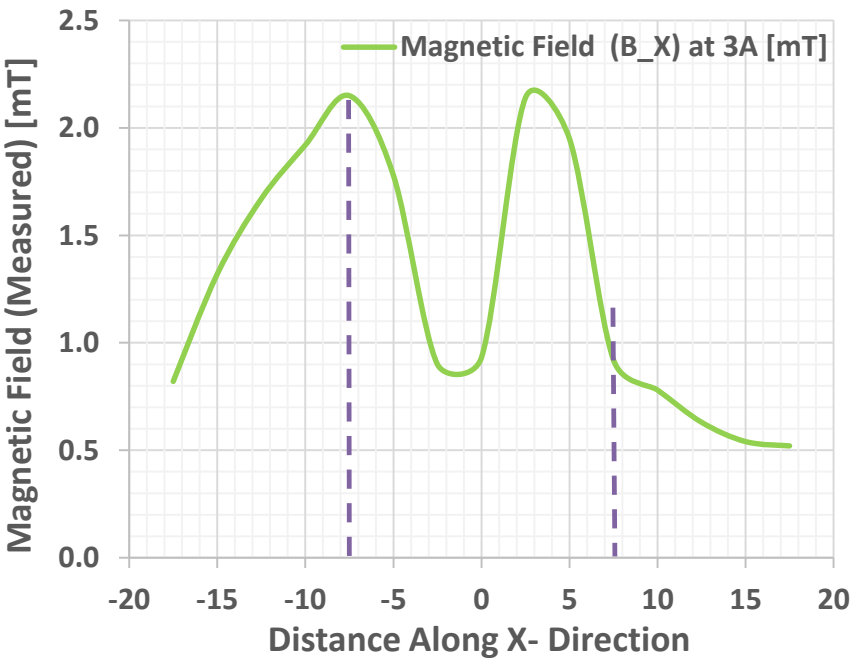

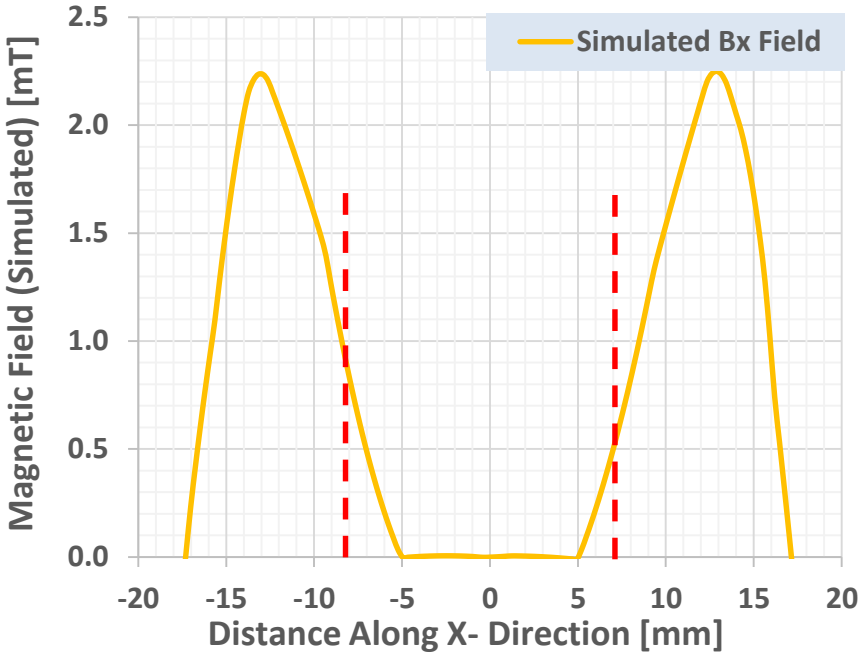

The region in between the dotted lines indicate where the actual defect is. In this region no field measurement is expected as the magnetic flux goes around the defect as there is very low magnetic permeability.

Simulated results show the expected curve. The experimental measurement curve, shows the existence of the defect (indicated by a shallow deep).

Fig 13. Bx Component DC Magnetic Field Measurement [left] and Simulated result [right]

DC Magnetic Field Experimental Test Results

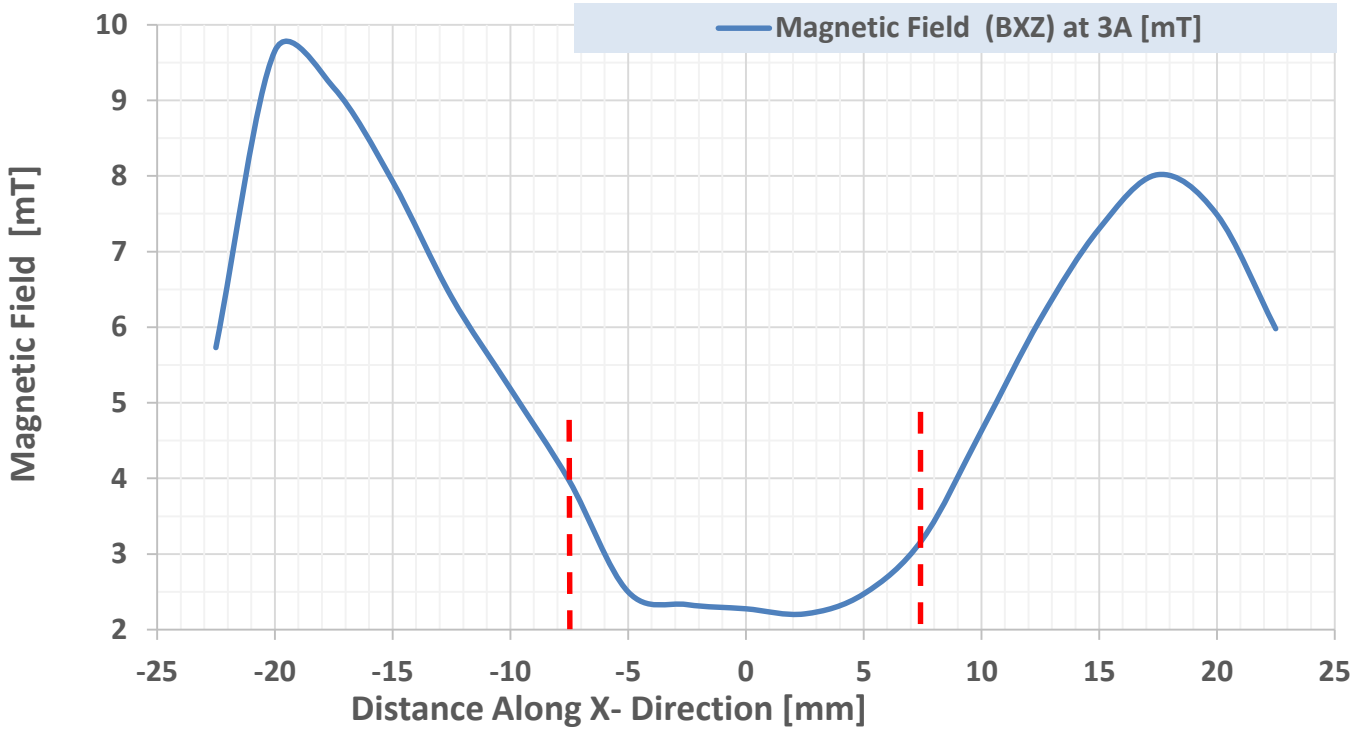

Fig 14. Combined curve, resultant of of Bx and Bz components

The graph above is generated taking the resultant of Bx and Bz, i.e., $(B_{XZ} = \sqrt{B_X{}^2 + B_Z{}^2})$. The region in between the **red** dotted lines indicate how wide the groove is.

While the defect is detected 'slightly' on the separately 'Measured Bx' and 'Measured Bz' curves, combining the two results in such a way can enhance defect detection and defect sizing. This approach can be implemented in the handheld scanner to both scan defects and estimate their dimensions.

AC Magnetic Field Experimental Test Results

Coil Parameters

- Wire diameter = 0.71mm (copper)
- Number of turns = 31 per layer
- Number of layers = 3

Test Material

- Material: Aluminium Sheet
- Through hole diameter = 20mm
- Grids shown = 10mm x 10mm

AC Magnetic Field Experimental Test Results

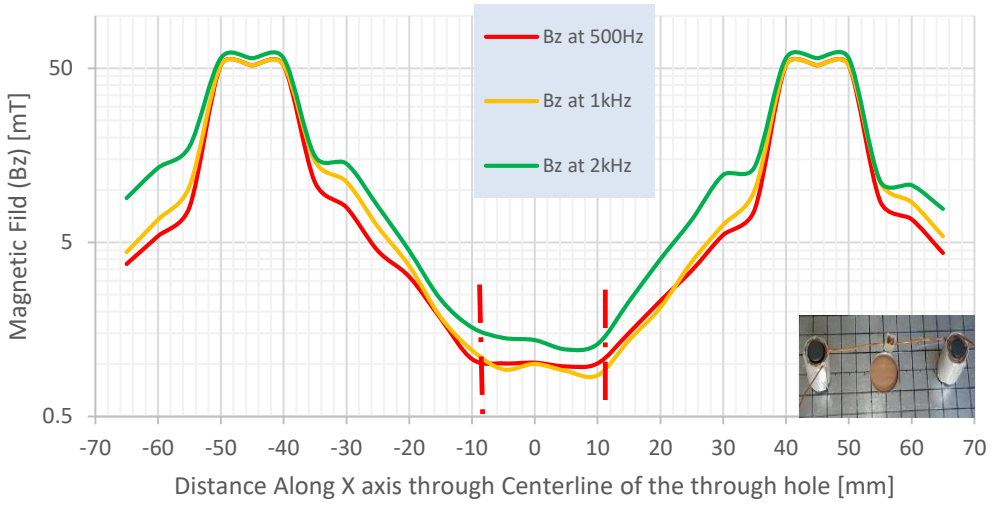

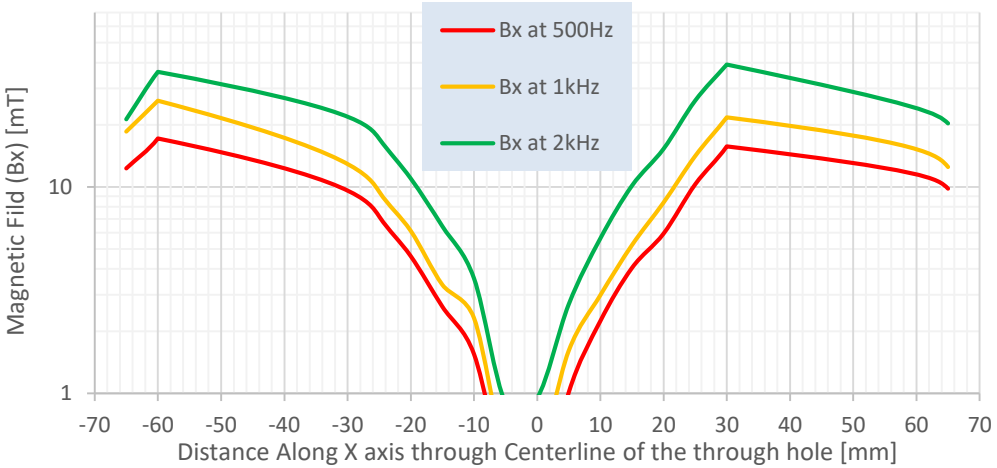

The B_z plot clearly shows the defect position, the region of plot shown between the dotted lines in the left figure indicates very close dimension of the through hole diameter.

B_x values at the center top of the 20mm through hole also drop to near zero as eddy currents make their way around it when they encounter the through hole.

As a result a weak magnetic field is registered at the center of the through hole pointing the existance of a ‘defect’

Fig 15. AC magnetic field experimental results of Bx and Bz components

AC Magnetic Field Experimental Test Results

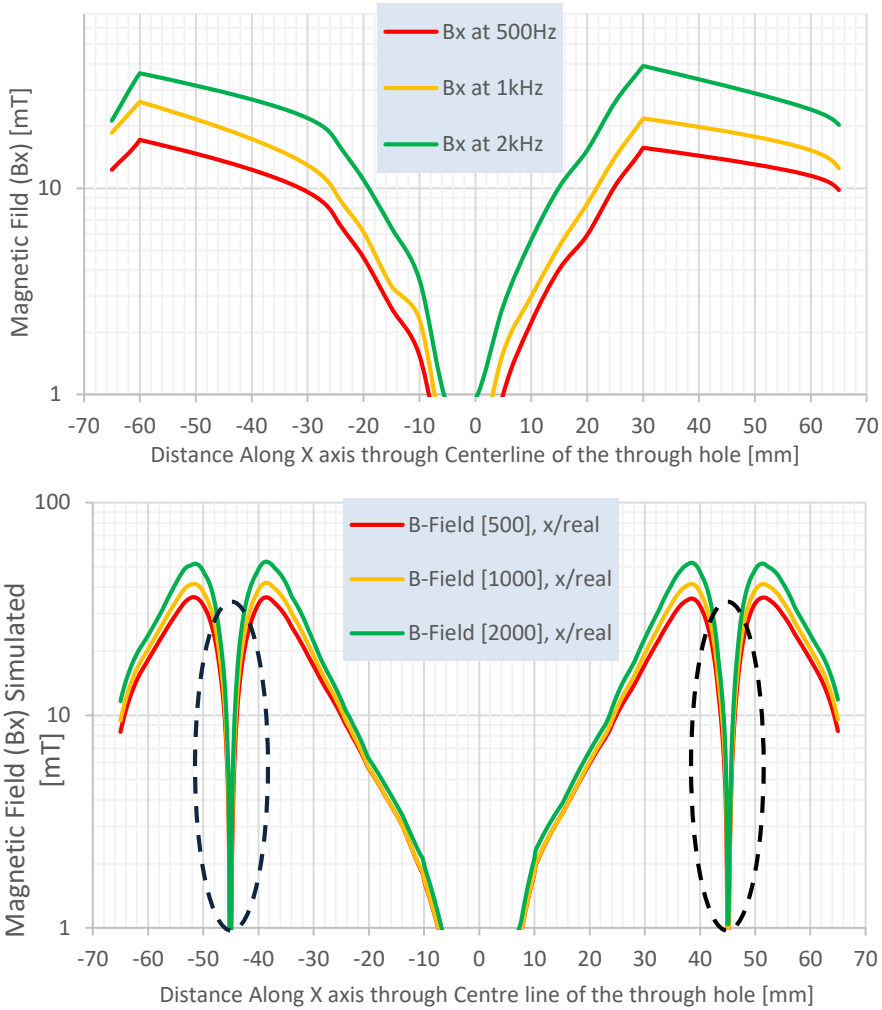

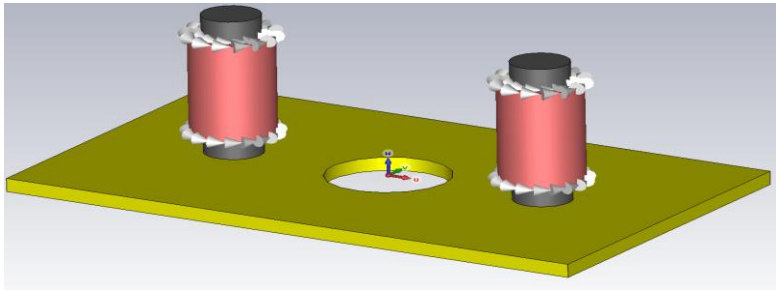

Significant difference of the simulated and measured result curves is that Bx measurement is not taken at the magnets location, as it is physically not possible but assumption of dominant Bz field is taken and Bx is set to zero. Rapid drop of Bx in the simulated result, shown in dotted ellipses, support this claim.

Measurements show close resemblance with simulated results promising continual improvement in measurement and data processing for more accurate defect detection by QWHE sensors

Fig 16. AC magnetic field comparison of experimental and simulated results

Magnetic Field Reversal Test Using HHS

- Magnetic field reversal from ‘south’ magnetic pole to ‘north’ where the curve intersects zero, is shown on both vertical and horizontal sensor arrays
- The deep spot in the ‘Combined’ curve at 15mm position indicates where the field reversal takes place

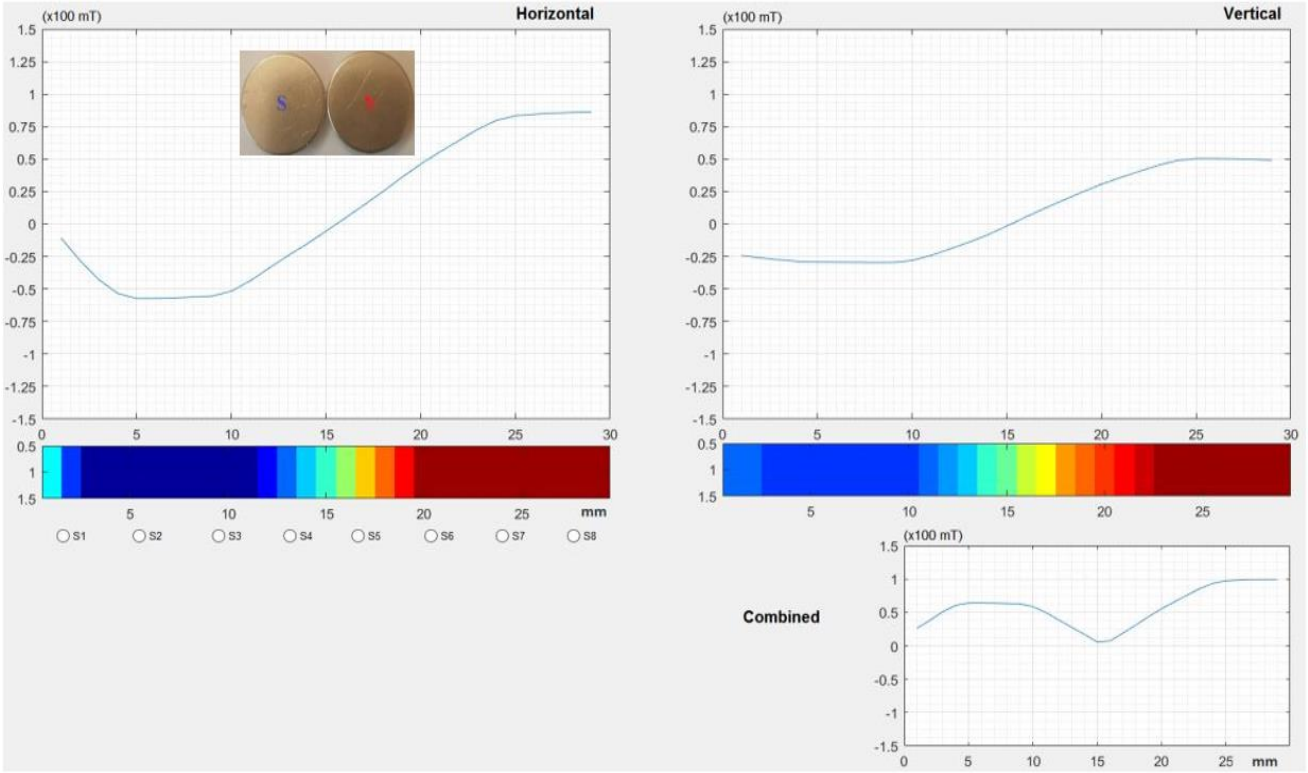

Fig 17. Initial test of the handheld scanner for magnetic field reversal

MANCHESTER 1824
The University of Manchester

Summary

- A QWHE sensor based handheld scanner utilizing two arrays of such sensors was successfully designed and built.
- Preliminary tests have been carried out out to verify that the device was working properly and successful preliminary results are reported.
- A programmable electromagnetic coil was designed and is in its programming and testing stages.
- Future improvement include programmable electromagnetic coils and programming stages so that it can be used to illuminate both DC and AC magnetic field from on board power source.
- The handheld scanner will play important roles in speeding up testing at increased sensitivity.

MANCHESTER 1824
The University of Manchester

Thank You

The project is part funded by EPSRC and STFC for which the authors are very grateful

(STFC-ST/L000040/1 “HIGH RESOLUTION 2D MAGNETIC VISION-B-CAM” and EPSRC-EP/LO22125/1 “UK RESEARCH CENTE IN NON-DESTRUCTIVE EVALUATION (RCNDT)”)